DOI: https://doi.org/10.5592/CO/EUROENGEO.2024.131

KINEMATIC AND BLOCK THEORY ANALYSIS IN DOLOMITIC ROCKMASS FOR DAM-SITE STABILITY

SANJEEV REGMI[1], RANJAN KUMAR DAHAL [2]

[1] *Nepal Electricity Authority, Dudhkoshi Jalvidhyut Company Ltd, Kathmandu, Nepal, regmisanjeev@gmail.com*

[2] *Central Department of Geology, Tribhuvan University, Kirtipur, Kathmandu, Nepal, rkdahal@gmail.com*

Abstract

In the realm of dam-site slope stability assessments, an integrated approach utilizing both kinematic and block theory offers robust and comprehensive insights. Although, each theory possesses its advantage and limitations, the combined approach yields a more holistic understanding of potential failure mechanisms and formulating risk mitigation strategies. Kinematics analysis evaluates the potential movement of individual rock blocks within the rockmass, based on the orientation and properties of discontinuities whereas block theory analyses their stability due to exposed condition. This is the primary concern, ensuring the dam's slope whether rockmass could withstand without failure or excessive deformations that could compromise its integrity. This study is concentrated on dolomitic rock type and hence it considers the possible kartification dissolution, weathering and variable mechanical properties in such rock type. The geological model was prepared from geological study and eight scan lines were drawn on each bank of Dam-site of Tanahu Storage Hydroelectric Project. It was later verified with finite element analysis method. It was concluded that the maximum safe slope for dam-site slope is between 45 and 50 degrees. There was slope deformation on the right bank of the Dam-site after excavation. Hence, slope excavation should be conducted after considering safe slope for gaining required slope stability of the area.

Key words

Kinematic and Block Theory Analysis, dolomitic rock type, karst topography, finite element analysis method, maximum safe slope.

1 Introduction

In the realm of dam-site slope stability assessments, an integrated approach utilizing both kinematic and block theory offers robust and comprehensive insights (Liang et al., 1999), (Gurocak et al., 2008) and (Kulatilake et al., 2011). Block theory is a geometrically based set of analyses that determine where potentially dangerous blocks can exist in a geological material intersected by variously oriented discontinuities in three dimensions (Goodman, 1995) and (Wang & Ni, 2014). It applies ideally to hard, blocky rock in which blocks of various sizes may be potential sources of load and hazard during construction. The rockmass condition is the main intrinsic factor that determines the probability of failure of rock so the proper assessment of actual condition is vital in rock engineering and designing infrastructures (Jaeger, 1979). The geometry of dam, such as its slope angle and thickness, is main concern as it resist the hydrostatic pressure and other forces (Adamo et al., 2020). In other hand, geology of foundation of dam and permeability condition of ground are primary concerns during (Cambefort, 1977) (Warner, 2004) investigation period. All these factors plays crucial role in dam safety.

The mechanical and chemical properties of the bedrock affects the stability of slope highly (Wahlstrom, 2012). The fractured and jointed rockmass of dolomite is vulnerable to karst formation if rockmass gets exposed to ground water (Abdullatif, 2010) and Gauri & Bandyopadhyay, 1999). The proper investigation is required for the identification of rockmass properties and in-situ conditions. This works

includes studies of its geological factors like joint orientation, spacing, rockmass strength, deformability, weathering, erosion and groundwater conditions.

The aim of the present study is to apply integrated approach of kinematic and block theory for the slope assessment of dam-site in Tanahu Storage Hydroelectric Project. It is further verified by simulation works using Rocscience's Phase -2.

The project consists of a concrete gravity dam with a maximum height above foundation level of 140m. The project is located in Tanahu district of Gandaki state (State no 4) of Nepal as shown in Fig1. The major structures of the project are located on the right bank of the Seti River and Madi River. The dam-site of the project lies on the Hatisude and the powerhouse area lies on Bateni.

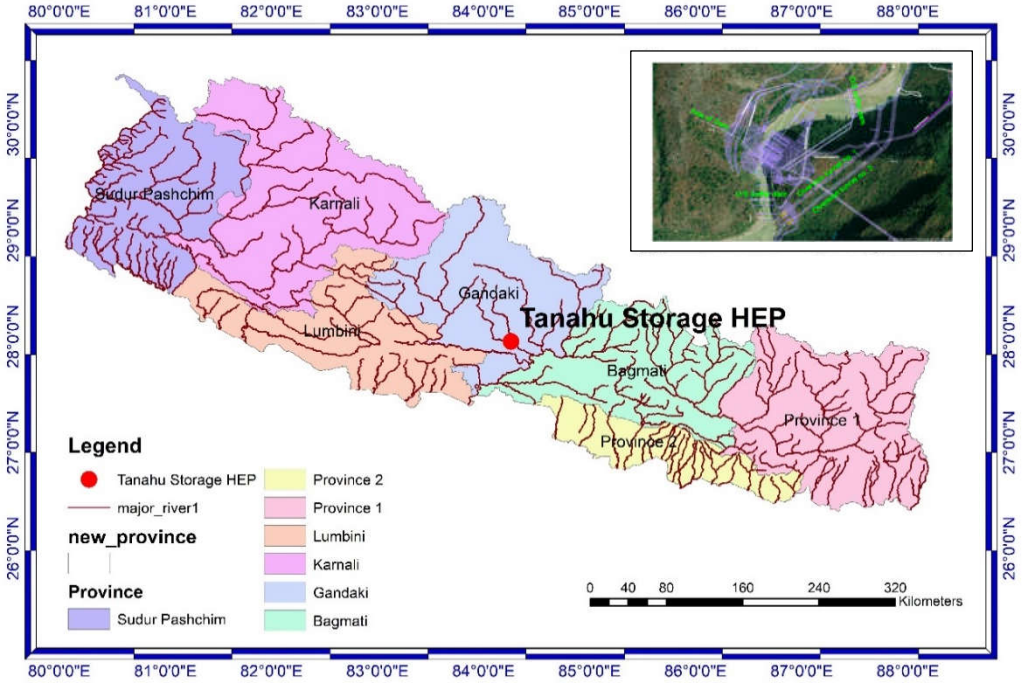

Figure 1. Location map of Tanahu Storage Hydroelectric Project

The predominant lithology of the area is Benighat Slate and Dhading Dolomite of Palaezoic to Precambrian belonging to Nawakot group. The massive dolomite is intercalated with thin bed of dark gray colored slate in dam-site area. The dam – axis is mainly consisting of thickly foliated, massive, yellowish colored, fractured, slightly weathered dolomite. Dolomite is well exposed along the Seti river bank on the dam-site area. The general trend of the bedrock is 340° to 10°. Benighat Slate which overlains the dolomitic rockmass, consists of dark bluish-gray to black, soft weathering, and highly cleaved slates and phyllites. The slate is abundant on the elevation of 500 amsl.

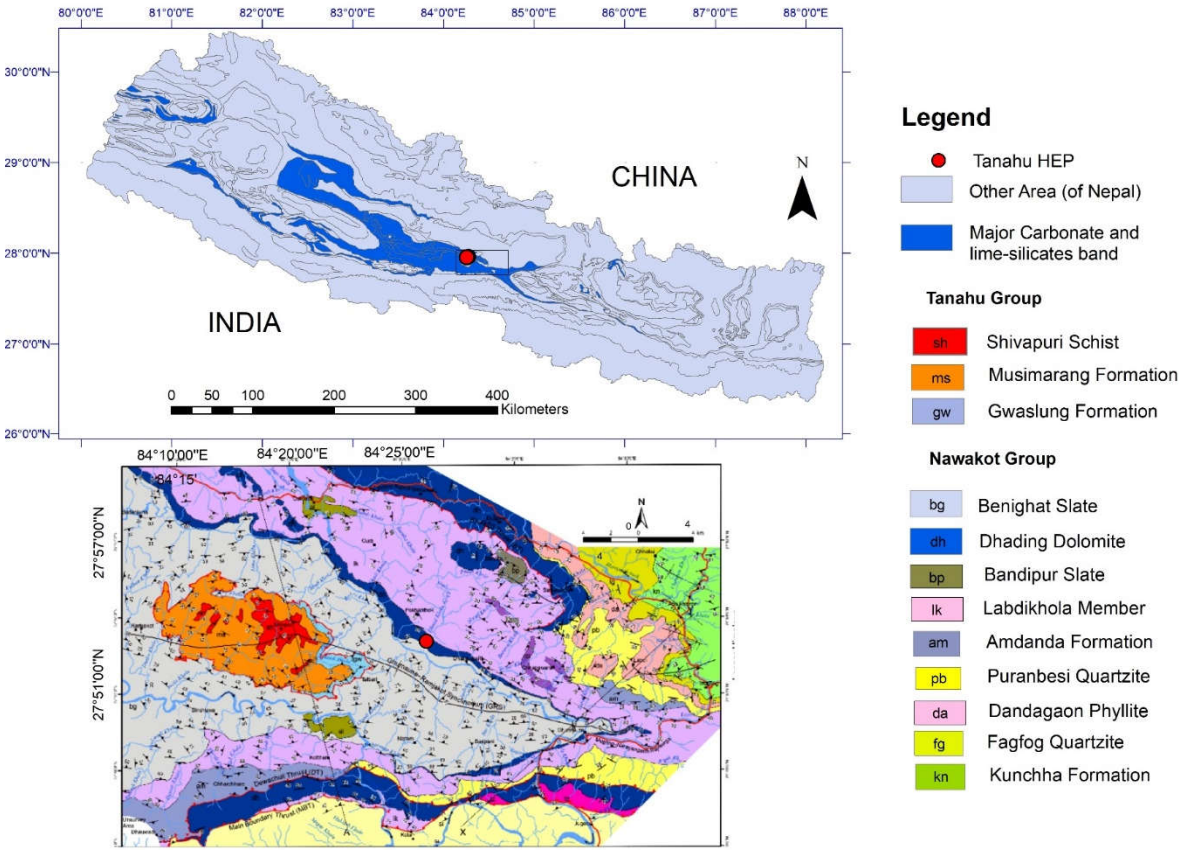

Figure 2. Regional Geological Map of Damauli (after Dhital, 2014 and Paudyal and Paudyel 2013)

2 Methods

Block theory and kinematics analysis are applicable for finding out possible failures and determining Maximum Safe Slope Angle (MSSA) of rock slope (Goodman, 1976). In this study, altogether eight profiles with four profiles on each bank were taken on the hillslope of dam-site area. However, 50 joints for each scanline, which most represented the ground conditions, were processed utilizing a commercially available software DIPS 7.0 (Rocscience, 2017), based on equal angle stereographic projection and major joint sets and analysed with respect to the attitude of discontinuity. During this process, the blocks were categorized into finite (completely bounded by discontinuities) or infinite (extending to the rock mass boundary). The evaluation of potential blocks movements was analysed with respect to the orientation of discontinuities and the excavation geometry which provides insight to determine whether blocks could slide or fall under gravity or external forces. In addition, Phase-2 (Rocscience, 2017) was used to simulate the hillslope of the dam.

2.1 Kinematics Analysis

More than 500 representative joint-sets were collected from the study area for kinematic analysis of discontinuities. The analysis is related with the geometry of discontinuities in rockmass with respect to cut slope. The equal angle stereographic projection was applied during the analysis. Plane, wedge and toppling failure mode were identified. These failure modes were calculated on the different possible slope of cut direction with varaiable dip amount. The Table 1 shows the properties of selected scanline at the dam-site.

Table 1. Properties of selected Scanlines at the Dam-site

Scanline Number	Location	Rock face Dip Dir/Dip Amount(°)	Scanline trend/Plunge(°)	Rock Mass
LD-1	Weir	107/70	115/0	Fair
RD-1	Weir	300/52	295/0	
LD-2	Dam-Axis	115/56	110/0	Fair
RD-2	Dam-Axis	300/56	290/0	Fair
LD-3	U/S Dam-Axis	080/46	095/0	Fair
RD-3	Intake	265/55	270/0	Fair
LD-4	U/S Dam-Axis	128/35	115/0	Fair
RD-4	Diversion Inlet	240/45	260/0	Fair

2.2 Block Theory Analysis

The blocks that were formed due to joint's orientation, natural hillslope and cutslope were categorized into infinite block, finite (non-removable block), finite (removable block but stable without friction), finite removable block (stable with sufficient friction) and finite, removable block unstable without support). The factor of safety of block was analysed by SWEDGE (2017). There were three prominent discontinuities in selected eight scanlines. The aim of the block theory analysis is to find out the MSSA of the respective block of the scanline. The representative discontinuity is actually the mean of the discontinuity orientation and different cut slope direction that were determined as per possible cutslope for the selected scanline.

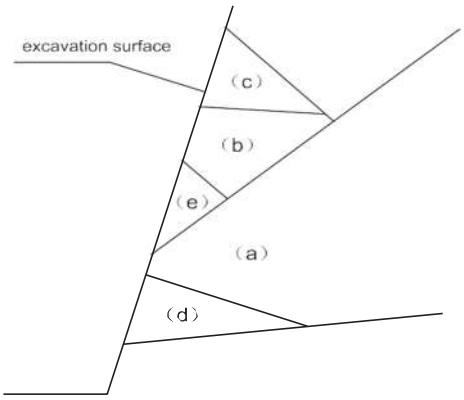

•Infinite
•Finite, nonremovable, tapered
•Finite, removable stable without friction
•Finite, removable, stable with sufficient friction
•Finite, removable unstable without support

Figure 3. Types of blocks in a surface cut infinite (type V block), tapered (type IV block), stable (type III block), potential key block (type II block), and key block (type I block).

2.3 Finite Element Method

A continuum approach of Finite Element Method is the most used approach for numerical modelling of hillslope. In this approach, the rockmass is meshed applying elements of triangular or quadrilateral shape in 2D. The fixed boundary condition was adopted for the simulation except cutslope area. The failure criterion of intact rock which has been developed by Hoek-Brown (Hoek & Brown, 1980) was applied for simulation. The equation of the failure of intact rock is shown in Eq. (1):

$$\sigma 1 = \sigma 3 + \sqrt{mi\frac{\sigma 3}{\sigma c} + 1} \quad (1)$$

where σc is the Uniaxial Compressive Strength (UCS) of the material and mi is a material constant which defines the brittleness of intact rock. In this equation, $\sigma 1$ and $\sigma 3$ are major and minor principal stresses respectively, that act on the rockmass and are used to define the rock mass failure envelope in the Hoek –Brown failure criterion. This criterion allows simulation of varied stress-strain behaviour from simple elastic to elasto-plastic or time-dependent creep. This method can give information about the deformations at working stress levels and is able to monitor progressive failure including overall shear failure (Griffiths & Lane, 1999). Similarly, the Mohr Coulomb failure criterion was used for simulation of colluvial deposits. It is commonly used in geotechnical engineering to predict the behaviour of soils and rocks, but it can be also used for other materials. The criterion is based on the principal of maximum shear stress. According to this principle, a material will fail when the maximum shear stress on any plane within the material reaches a critical value. The Mohr - Coulomb failure criterion is expressed mathematically as shown in Eq. (2)

$$\mathrm{r} = c + 6n * \tan(\varphi) \quad (2)$$

Where r is the maximum shear stress on a plane within the material c, $6n\ and\ \varphi$ are cohesive strength of material, normal hear stress acting on the plane and the angle of friction between the particles of the material respectively. A Geological Strength Index (GSI) is used in conjunction with other parameters such as the rock quality (Q) and the rock mass rating (RMR) to evaluate the stability of a rock mass. A modification in the GSI approach was proposed for tectonically disturbed flysch rock masses (Hoek & Brown, 2019) and (Marinos & Hoek, 2000). In this study, the strength reduction method (SRM) was used to do this case study ((Fu & Liao, 2010) and (Hoek & Brown, 2019). The equations for calculating the rock mass with constants mb, s and a is in Eq. (3), Eq. (4) and Eq. (5).

$$m_b = m_i \exp\left(\frac{GSI-100}{28-14D}\right) \quad (3)$$

$$s = exp\left(\frac{GSI-100}{9-3D}\right) \quad (4)$$

$$a = \frac{1}{2} + \frac{1}{6}\left(e^{-GSI/15} - e^{-20/3}\right) \quad (5)$$

whereas D is a factor that depends upon the degree of disturbance to which the rock mass is subjected to blast damage and stress relaxation tests. In this study, the value of D is considered as zero.

3 Results

3.1 Kinematics Analysis

There are three different failures modes that have been identified in RD-2 region as shown in Table 2. The calculated final MSSA including and excluding toppling failure are between 45° and 60° and between 70° and 45° respectively at cut slope dip directions 95–290°. Similarly, the MSSA for plane sliding, wedge sliding and toppling failure and the final MSSA for the other seven regions were calculated, including and excluding toppling failure, selecting appropriate scanline orientation data from Table 2 with the kinematic analysis.

Table 2. MSSA for three basic failure modes under different possible cut slope dip directions at RD-2 region

Cut Slope Direction	MSSA for plane sliding			MSSA for Wedge			MSSA for Toppling			Dominant Mode		Final MSSA	
	D1	D2	D3	I1I2	I2I3	I3I1	T1	T2	T3	Including Toppling	Excluding Toppling	Including Toppling	Excluding Toppling
95	72	70	90	90	60	90	90	90	90	*D1,D2, I2I3*	*D1,D2*	60	70
110	72	70	90	90	50	90	90	90	90	*D1,D2, I2I3*	*D1,D2*	50	70
115	72	70	90	90	50	90	90	90	90	*D1,D2, I2I3*	*D1,D2*	50	70
125	72	70	50	90	45	90	90	45	90	*D1,D2, D3, I2I3,T2*	*D1,D2,D3*	45	50
260	72	70	50	90	45	90	90	90	90	*D1,D2,D3,I2I3*	*D1,D2,D3*	45	70
270	72	70	50	90	90	90	90	90	90	*D1,D2,D3,I2I3*	*D1,D2,D3*	50	50
280	50	50	60	90	90	90	90	90	90	*D1,D2,D3,I2I3*	*D1,D2,D3*	50	50
290	72	70	50	90	90	90	90	90	90	*D1,D2,D3,I2I3*	*D1,D2,D3*	50	50

Table 3. MSSA for three basic failure modes under different possible cut slope dip directions at LD-2 region

Cut Slope Direction	MSSA for plane sliding			MSSA for Wedge			MSSA for Toppling			Dominant Mode		Final MSSA	
	D1	D2	D3	I1I2	I2I3	I3I1	T1	T2	T3	Including Toppling	Excluding Toppling	Including Toppling	Excluding Toppling
95	90	90	90	90	90	90	90	90	90			90	90
110	90	90	90	90	90	90	90	90	90			90	90
115	90	90	90	90	90	90	90	90	90			90	90
125	90	90	90	90	90	90	90	90	90			90	90
260	90	90	90	90	77	90	90	90	90	*I2I3*		77	90
270	90	90	90	80	72	90	90	90	90	*I1I2, I2I3*		72	90
280	90	90	90	80	68	90	90	90	90	*I1I2, I2I3*		68	90
290	90	90	90	79	65	90	90	90	90	*I1I2, I2I3*		65	90

In Table 3, the MSSA is claculated for three different failure modes at LD-2 regions of dam-axis. The calculated final MSSA including and excluding toppling failure range between 65° and 90°.

Table 4. Percentage number of possible failure under each mode of instability for different slope regions

Region	Possible Cut-slope Dip Direction Range	Slope Ratio Vertical/Horizontal	Plane Sliding			Wedge Sliding			Toppling Failure		
			1:1	1:0.70	1:0.48	1:1	1:0.70	1:0.48	1:1		1:0.70
		Slope Angle (°)	45	55	65	45	55	65	1:0.48 45	55	65
LD-1	90-100		0.00	2.00	3.00	0.00	7.69	13.97	7.84	13.73	13.73
LD-1	110-125		0.00	1.96	5.88	0.31	5.73	13.43	11.76	17.65	21.57
LD-2	90-125		0.00	0.00	1.89	0.00	0.22	0.80	18.87	18.87	18.87
LD-2	260-290		0.00	0.00	0.00	0.00	0.29	4.73	18.87	18.87	18.87
RD-1	260-270		0.00	0.00	3.92	0.00	1.26	4.23	27.45	29.41	33.33
RD-1	280-290		0.00	1.96	3.92	0.00	1.97	6.05	27.45	29.41	33.33
RD-2	260-270		0.00	0.00	0.00	0.00	0.00	0.43	14.29	14.29	14.29
RD-2	280-290		0.00	0.00	0.00	0.00	0.00	0.00	6.12	6.16	6.16
LD-3	90-100		0.00	0.00	7.14	0.13	3.12	6.12	12.50	17.86	26.78
LD-3	110-125		0.00	3.57	8.93	0.00	3.71	13.85	16.07	25.00	33.43
LD-4	90-100		0.00	2.53	3.80	0.10	2.24	4.97	11.39	18.98	20.25
LD-4	110-125		0.00	0.00	0.00	0.00	1.01	3.11	17.72	25.31	30.38
RD-3	260-270		0.00	0.00	0.00	0.00	0.08	0.41	14.00	14.00	14.00
RD-3	280-290		0.00	0.00	0.00	0.00	0.08	0.16	6.00	8.00	8.00
RD-4	260-270		0.00	0.00	4.00	0.08	0.49	2.70	30.00	32.00	36.00
RD-4	280-290		0.00	0.00	2.00	0.00	0.16	4.25	24.00	24.00	30.00

The percentage of the possible plane sliding, wedge sliding and toppling sliding for discontinuities were obtained using Dips software of rocscience. Toppling failure percentage is maximum that is 36% in RD-4 scanline at cutslope direction 280-290° and slope angle 65°. In RD-2, the percentage of toppling failure in cutslope angle 65°, 55° and 45° is 33.33%, 28.41% and 27.45% respectively (Table 4). The cut slope direction varies between 280° and 290° in RD-2.

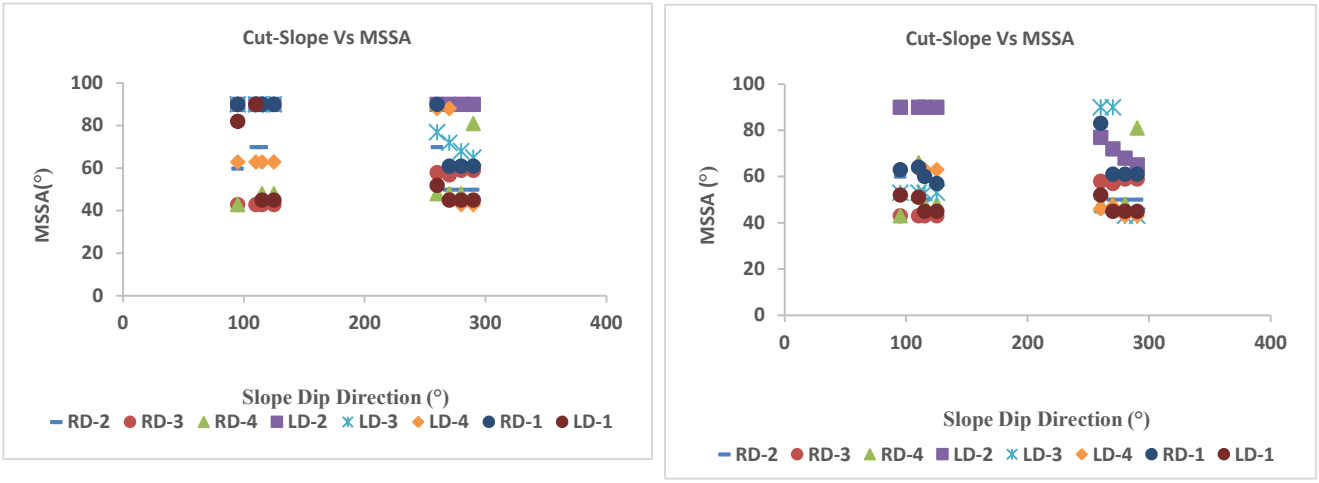

Figure 4. The relationship between MSSA (°) with Slope Dip Direction (°) including and exluding toppling failure.

The results given in Figure 4(a) and Figure 4(b) exhibits clearly that the final MSSA excluding toppling failure and including toppling failure is similar for slope direction between 95° and 125°. In the same region, the final MSSA including toppling failure is slightly lower in comparison to excluding toppling failure for slope direction between 260° and 290°. The final MSSA will range between 43° and 90° for wide range of slope direction between 95° and 290°, if other factors like the slope region, rock mass type and with or without toppling failure are not considered. The selected scanline with cut slope direction and cut slope angle for representative discontinuities the above results are obtained.

3.2 Block Theory Analysis

The block theory analysis was carried out in two region RD-2 and LD-2, which represents right and left slope of the Dam-site on three representative joint sets as tabulated in Table 2 only two discontinuities could be calculated at one time (Kulatilake et al., 2011). For the respective cutslope direction, key-block (type I block), sliding blocks and Type III block (stable block) were identified as shown in Table 5 and Table 6. In LD-2 region and RD-2 regions, possible slope direction ranges between 260° - 290° and 095° - 290° respectively. The factor of safety of key-blocks S23 and S12, which were formed in region LD-2 due to excavation, were greater than one and hence they were stable. Similarly, only one key - sliding block S23 was depicted in RD-2 which was unstable for the cutslope direction 095° and dip amount 70°. The clarity of three discontinuities is comparatively less than four and five discontinuities. It could be taken as the limitation of the study. However, analysis were carried out carefully so it actually represents the ground condition.

Table 5: Final failure modes and corresponding MSSA for different slope dip directions at LD2 region

Cut Slope Dip Dir. (°)	Discontinuity Combination	Key-block sliding mode	Potential key block	Type III block	Case MSSA	Final MSSA	Key block (sliding mode, safety factor)
260	*J1,J2,J3*	011(S23,77)		100	90	77	011(S23, >1)
	J1,J2 J3		110 (S12)	001	90		
	J1,J2,J3		101(S31)				
270	*J1,J2,J3*	110(S12,72)		100		72	110(S12, 3.4)
	J1,J2J3	011(S23,72)		001		72	011(S23, >1)
	J1,J2,J3		101(S31)		90		
280	*J1,J2,J3*	110(S12,68)		100		68	110(S12, 3.9)
	J1,J2,J3	011(S23,68)		001		68	011(S23,>1)
	J1,J2,J3		101(S31)		90		
290	*J1,J2,J3*	110(S12,65)		100		65	110(S12,3.3)
	J1,J2,J3	011(S23,65)		001		65	011(S23,>1)
	J1,J2,J3		101(S31)		90		

Table 6: Final failure modes and corresponding MSSA for different slope dip directions at RD2 region

Cut Slope Dip Dir. (°)	Discontinuity Combination	Key-block sliding mode	Potential key block	Type III block	Case MSSA	Final MSSA	Key-block (sliding mode, safety factor)
095	*J1,J2,J3*		110(S12)	100	70		
	J1,J2 J3	011(S23,60)		010			011(S23,0)
	J1,J2,J3		101(S31)		70		
110	*J1,J2,J3*			100	70		
	J1,J2J3	011(S23,50)		010	70	50	011(S23,>1)
	J1,J2,J3						
125	*J1,J2,J3*			100			
	J1,J2,J3	011(S23,45)		010,010	50, 45	45	011(S23,>1)
	J1,J2,J3			001			
260	*J1,J2,J3*		110(S12)	100	72		
	J1,J2,J3	011(S23,45)		010	70	45	011(S23,>1)
	J1,J2,J3		101(S31)	001	50		
270	*J1,J2,J3*		110(S12)	100	72		
	J1,J2,J3	011(S23,50)		010, 010	70, 90	50	011(S23, >1)
	J1,J2,J3		101(S31)	001	50		
280	*J1,J2,J3*		110(S12)	100	50		
	J1,J2,J3	011(S23,90)		010, 010	50	50	011(S23,>1)
	J1,J2,J3		101(S31)	001	60		
290	*J1,J2,J3*		110(S12)	100	72		
	J1,J2,J3	011(S23,90)		010, 010	70	50	011(S23,>1)
	J1,J2,J3		101(S31)	001	50		

3.3 Finite Element Analysis

The physical parameters of colluvial deposits, fractured rockmass and dolomite were carefully selected for simulation. The laboratory tests of the bedrock including UCS and Point Load Test (PLT) were extracted from the laboratory tests of samples and geotechnical investigation report of Tanahu Storage Hydroelectric project of Nepal Electricity Authority (Table 1). The simulation of Phase2 was carried out in the right bank of the dam-site in RD-2 region. After excavation, the strength factors of rockmass is reduced below 1 at the upper and bottom of hillslope.

Table 7: Physical and Mechanical Parameters used for Simulation

	GSI	Hoek - Brown Parmeters				Deformation Modulus (GPa)	Poisson's Ratio	Internal Friction Angle (°)	Cohesion (MPa)
		m_i	m_b	s	a				
Massive Dolomite	70	12	1.408	0.0067	0.501	15	0.2	50	3.8
Fractured Dolomite	60	10	0.57	0.0013	0.503	2.5	0.3	40	1.8

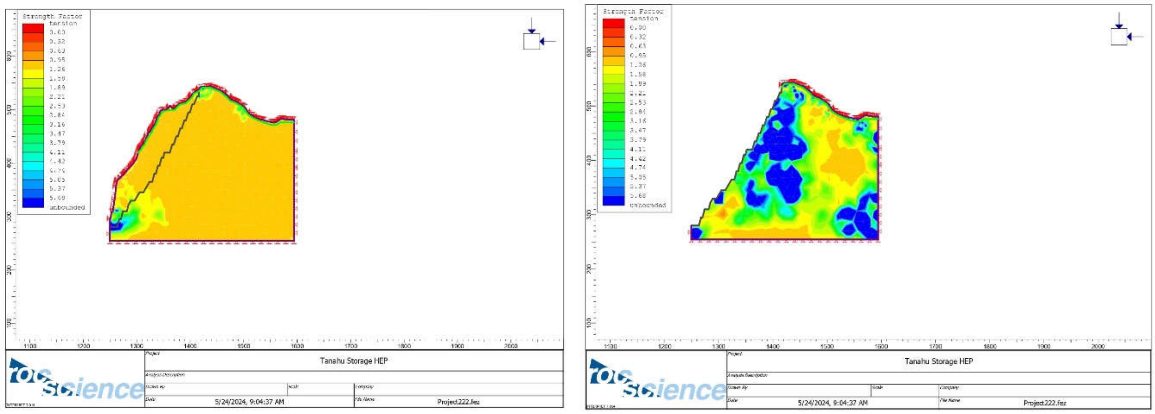

Figure 5. Strength Factor in the Right Bank of Hill-slope of Dam without excavation and with excavation

4 Conclusion

In this study, geological information were collected from field investigations, laboratory tests and other lithological information from report and literature. The dam-site belongs to Dhading Dolomite which is is characterized by thickly bedded structured to massive structured; rock is moderate to strong fracture. The predominant dip direction of discontinuities are NNE, NWW and SWW with dip amount varies between 25° and 65°. Three prominent discontinuities were thoroughly studied by identifying eight scanline from both sides of dam-site for kinematics and block theory analysis. The rock types encountered in left side is comparatively stronger, less fractured and more stable than right side. The friction angle of Dolomite is between 42° and 45°.

In this study, the output of MSSA from kinematics analysis matches with MSSA acquired from block theory analysis. The block theory analysis identifies two key blocks S12 and S23 for LD-2 region and final MSSA of cutslope direction 260°, 270°, 280° and 290° are 77°, 72°, 68° and 65° respectively. However, only one key block S23 is depicted for sliding mode. Along cut slope direction 095°, key block shows possible failure at dipping angle 60°. The final MSSA ranges between 45° and 50°. Toppling failure percentage is maximum that is 36% at RD-4 with cutslope 280-290° (dip direction) and slope angle 65°. The scanline RD-2 where we could observe displacement after excavation (Table 12) exhibits 33.33%, 28.41% and 27.45% toppling failure for cutslope angle 65°, 55° and 45° respectively for cut slope direction 280-290°.

The simulation of Phase2 was carried out in the left bank of the Dam-site in RD-2 scanline. After

excavation, the strength factor of hillslope is below 1 at the upper and bottom of hillslope. Hence, careful excavation with necessary support measures is required in regions namely RD-1, RD-2, RD-3 and RD-4.

Acknowledgements

This research has been conducted with the extensive help from professional and academicians, involved in hydropower projects. Authors are thankful to Nepal Electricity Authority for helps and supports.

References

Abdullatif, O. (2010). Geomechanical properties and rock mass quality of the carbonate Rus formation, Dammam dome, Saudi Arabia. *Arabian Journal for Science and Engineering*, *35*(2), 173.

Adamo, N., Al-Ansari, N., Sissakian, V., Laue, J., & Knutsson, S. (2020). Dam safety: General considerations. *Journal of Earth Sciences and Geotechnical Engineering*, *10*(6), 1–21.

Cambefort, H. (1977). The principles and applications of grouting. *Quarterly Journal of Engineering Geology and Hydrogeology*, *10*(2), 57–95.

Fu, W., & Liao, Y. (2010). Non-linear shear strength reduction technique in slope stability calculation. *Computers and Geotechnics*, *37*(3), 288–298.

Gauri, K. L., & Bandyopadhyay, J. K. (1999). *Carbonate stone: Chemical behavior, durability, and conservation*. John Wiley & Sons.

Goodman, R. E. (1995). Block theory and its application. *Geotechnique*, *45*(3), 383–423.

Griffith, A. A. (1924). *Theory of rupture*. 55–63.

Griffiths, D., & Lane, P. (1999). Slope stability analysis by finite elements. *Geotechnique*, *49*(3), 387–403.

Gurocak, Z., Alemdag, S., & Zaman, M. M. (2008). Rock slope stability and excavatability assessment of rocks at the Kapikaya dam site, Turkey. *Engineering Geology*, *96*(1–2), 17–27.

Hoek, E., & Brown, E. (2019). The Hoek–Brown failure criterion and GSI–2018 edition. *Journal of Rock Mechanics and Geotechnical Engineering*, *11*(3), 445–463.

Hoek, E., & Brown, E. T. (1980). Empirical strength criterion for rock masses. *Journal of the Geotechnical Engineering Division*, *106*(9), 1013–1035.

Hoek, E., & Diederichs, M. S. (2006). Empirical estimation of rock mass modulus. *International Journal of Rock Mechanics and Mining Sciences*, *43*(2), 203–215.

Jaeger, C. (1979). *Rock mechanics and engineering*. Cambridge University Press.

Kulatilake, P. H., Wang, L., Tang, H., & Liang, Y. (2011). Evaluation of rock slope stability for Yujian River dam site by kinematic and block theory analyses. *Computers and Geotechnics*, *38*(6), 846–860.

Liang, R., Nusier, b, OK, & Malkawi, A. (1999). A reliability based approach for evaluating the slope stability of embankment dams. *Engineering Geology*, *54*(3–4), 271–285.

Marinos, P., & Hoek, E. (2000). *GSI: a geologically friendly tool for rock mass strength estimation*. ISRM-IS.

NEA, 2014. Detailed Engineering Study of Tanahu (Upper Seti) Hydropower Project in Nepal

NEA, 2015. Final Report of Geotechnical Investigation.

NEA, 2021. Engineering Geological Report (Geological Assessment).

Um, J.-G., & Kulatilake, P. H. (2001). Kinematic and block theory analyses for shiplock slopes of the Three Gorges Dam Site in China. *Geotechnical & Geological Engineering*, *19*, 21–42.

Upreti, B. (1999). An overview of the stratigraphy and tectonics of the Nepal Himalaya. *Journal of Asian Earth Sciences*, *17*(5–6), 577–606.

Wahlstrom, E. (2012). *Dams, dam foundations, and reservoir sites* (Vol. 6). Elsevier.

Wang, S., & Ni, P. (2014). Application of block theory modeling on spatial block topological

identification to rock slope stability analysis. *International Journal of Computational Methods*, *11*(01), 1350044.

Warner, J. (2004). *Practical handbook of grouting: Soil, rock, and structures*. John Wiley & Sons.